

4–8 GHz Near-Field Probe for Scanning of Apertures and Multimode Waveguides

Ivan Russo, *Student Member, IEEE*, and Wolfgang Menzel, *Fellow, IEEE*

Abstract—In this letter, a high-resolution 4-to-8 GHz-matched dipole probe for near-field mapping of apertures and oversized waveguides is presented. Thanks to its high selectivity, the proposed structure is able to measure with high precision a single linear component of the E-field in the reactive near-field zone. Simulations and measurements of the reflection coefficient and of the field patterns of a horn antenna and an oversized waveguide are reported in the last section.

Index Terms—Dipole, field mapping, near-field, probe.

I. INTRODUCTION

HIGH resolution probes are key elements for those applications that involve near-field scan of an object to determine its geometrical or electromagnetic characteristics. For instance, referring to near-to-far field transformations [1], near-field imaging and mapping [2], the accuracy of the pattern strongly depends on the resolution as well as the polarization purity of the testing device during the scan.

Several probe types are reported in literature. Some probe configurations were shown in [3] to determine the EM field in proximity of some microstrip structures and it was proved that the spatial resolution of a dipole is half of its length. In [4], the three different rod, dipole and SIW probes were designed to characterize the near-field of a reflectarray at 35 GHz. The authors presented also a high resolution near-field probe with integrated illuminating waveguide operating at 77 GHz in [5].

The previous probes are, in general, relatively narrowband. Broadband high resolution imaging can be performed, at the cost of a more complex system, by using low-invasive electro-optical probes, as demonstrated in [6]. Broadband near-field probes can be also realized by means of ridged waveguides. In [7], a ridged waveguide probe showing a 120% bandwidth between 12 and 50 GHz with SWR smaller than three was demonstrated. On the other hand, waveguide probes have in general a relatively big transversal section that can represent a perturbation when scanning the near-field of apertures.

In this letter, a low-profile broadband dipole probe, matched from 4 up to 8 GHz, is presented. The structure is based on an UWB feed and series chip resistors for impedance matching purposes. The structure has been tested comparing the measured

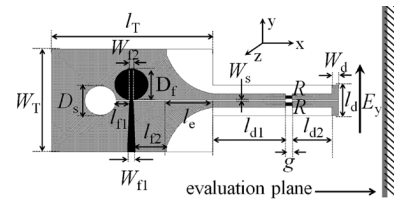


Fig. 1. Layout of the proposed broadband near-field probe.

field distributions of a horn antenna and oversized circular waveguide with the theoretical patterns. The structure shows fine resolution and good polarization purity, defined as the ratio between the desired and the undesired transversal components of the electric near-field pattern. Furthermore, thanks to the low profile of the probe, no relevant changes have been observed in the input reflection coefficient of measured DUTs.

II. PROBE ARCHITECTURE

The layout of the proposed probe is reported in Fig. 1. The dielectric substrate is Rogers RO4003 having $\epsilon_r = 3.38$ and thickness $h = 0.5$ mm. The probe is made of four main sections: a microstrip feed, a slotline section, a section of parallel strips and a short dipole. The microstrip and the slotline sections are interfaced through an UWB vertical transition similar to [8] followed by a taper to parallel strips that feed the dipole on the right side. Two series resistances R are used to improve the matching of the dipole to the parallel strips section.

III. PROBE DESIGN

The individual sections of the near-field probe have been optimized via full-wave simulations [9] to fulfill a -10 dB-matched operational bandwidth between 4 and 8 GHz.

A. Microstrip-to-Slotline Transition

The transition is used to transform, over the desired bandwidth, the $Z_f = 50 \Omega$ microstrip impedance to the $Z_s = 100 \Omega$ slotline impedance on the other side of the dielectric substrate. The two metal semi-planes forming the slotline after the transition are then tapered to a parallel strip transmission line with a strip-width 1 mm and slot-width W_s using a profile of length l_e with exponential coefficient $c = 0.35$. Table I summarizes the optimized dimensions of the transition.

B. Dipole Input Impedance Optimization

The dipole is the core element of the probe and must be able to provide high polarization purity, high resolution and good matching across the desired bandwidth. Referring to [3], the resolution can be considered as half the dipole length. To achieve

Manuscript received June 22, 2011; revised October 10, 2011; accepted October 13, 2011. Date of publication November 07, 2011; date of current version December 07, 2011.

The authors are with the Institute for Microwave Techniques – University of Ulm, Ulm 89081, Germany (e-mail: ivan.russo@uni-ulm.de; wolfgang.menzel@uni-ulm.de).

Color versions of one or more of the figures in this letter are available online at <http://ieeexplore.ieee.org>.

Digital Object Identifier 10.1109/LMWC.2011.2173324

TABLE I
 DIMENSIONS OF THE TRANSITION AND DIPOLE

W_T	l_T	W_{f1}	W_{f2}	D_f
17 mm	24.5 mm	1.2 mm	0.6 mm	5.1 mm
D_s	W_s	l_{f1}	l_{f2}	l_e
4.8 mm	0.2 mm	2 mm	5 mm	7 mm
W_d	l_d	l_{d1}	l_{d2}	g
1 mm	5 mm	11 mm	6 mm	1 mm

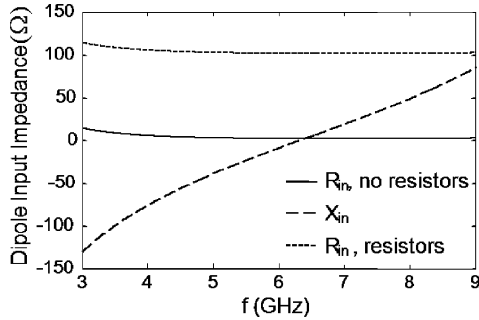


Fig. 2. Input impedance of the combination of quarter wavelength line and dipole with a zero of the reactance around 6 GHz. The two 50 Ω chip resistors transform the input resistance to 100 Ω , without any change in the imaginary part.

a desired resolution of at least 2.5 mm, the length of the dipole is chosen to be $l_d = 5$ mm. The dipole will be resonant at frequencies much higher than the operating frequency range. The short dipole is nearly an open end. Adding parallel strip of length $l_{d2} = \lambda_g/4$ at the center frequency, where λ_g is the wavelength of the parallel strip section, the input impedance can be transformed to nearly 0 Ω , as shown in Fig. 2. In this case, a relatively flat variation of the input impedance is expected. This behavior will help in achieving the broadband response from 4 GHz to 8 GHz. In fact, using two $R = 50$ Ω chip resistors connected in the gap g (Fig. 1), the input resistance of the combination of quarter wavelength line and dipole is transformed to the parallel stripline impedance $Z_s = 100$ Ω , without affecting the input reactance. In Table I, the optimized dimensions of the dipole are specified.

C. Dipole Resolution and Polarization Purity

The resolution of the probe can be defined in terms half-power beamwidth (HPBW) of the near-field pattern of the component \underline{E}_y , referring to the coordinate system in Fig. 1.

Full-wave simulations have been performed positioning the evaluation plane in the reactive near-field zone at a distance of 2 mm from the dipole. Fig. 3(a) reports the normalized amplitude of the \underline{E}_y component in dB along the y direction at the two limit frequencies 4 and 8 GHz. The simulated HPBW resolution is $\Delta \approx 2$ mm. The nulls in the \underline{E}_y -pattern are justified by the fact that the electric field is normal to the measurement plane in the proximity of the edges of the dipole, as depicted in Fig. 3(b). No relevant changes have been observed moving the measurement plane from 1 to 4 mm away from the probe. The near-field patterns along y and z of the undesired transversal component \underline{E}_z and longitudinal component \underline{E}_x have an odd symmetry with respect to the center of the probe. This is also true along the orthogonal z coordinate. If the probe is used

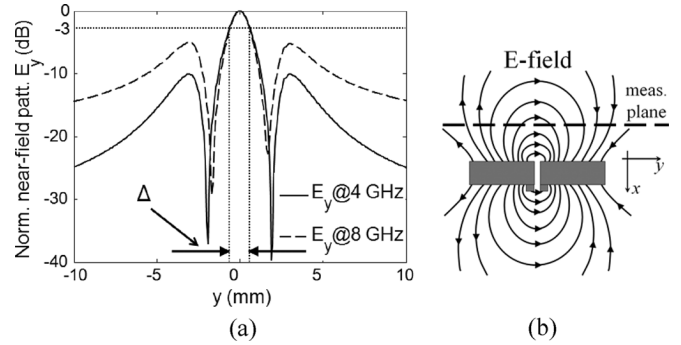


Fig. 3. (a) Simulated normalized near-field probe-pattern in dB along y at a distance of 2 mm from the dipole for the \underline{E}_y at 4 and 8 GHz; (b) Near-field electric lines for a short dipole.

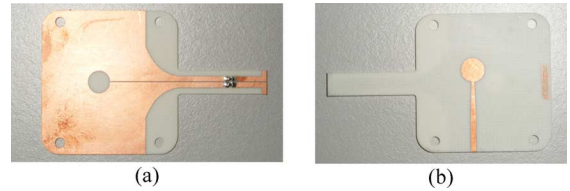


Fig. 4. Manufactured probe: (a) Top view; (b) Bottom view.

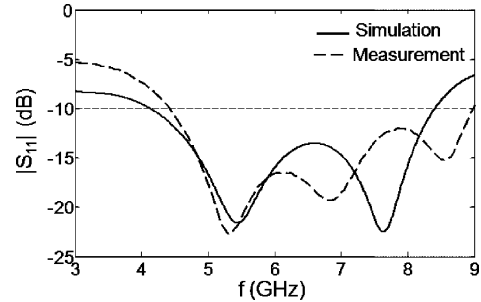


Fig. 5. Simulated and measured reflection coefficient at the probe feed.

to scan transversal sections having relatively slow gradient variations of the field amplitude, as usual for multimode waveguides or apertures, the contributions \underline{E}_z and \underline{E}_x are actually cancelled out or strongly reduced by the odd-symmetry property. For this reason, the dipole probe is able to accurately sense only the desired \underline{E}_y . The polarization purity, estimated through full-wave simulations and defined as E_y/E_z , shows values between 47 dB and 30 dB from 4 to 8 GHz at the center of the probe.

IV. SIMULATION AND MEASUREMENT RESULTS

Full-wave simulations and measurements of the manufactured probe (Fig. 4) have been carried out in order to characterize its performances.

Simulation and measurement of the input reflection coefficient are reported in Fig. 5, which shows how the device is well matched across the frequency range 4–8 GHz, with an S_{11} parameter always lower than -10 dB.

The probe has been also characterized in terms of near-field scanning capability. Two test structures have been measured through scanning on a rectangular grid: a C-band horn antenna having an aperture area of (152×113) mm² and a hollow oversized waveguide having a diameter of 160 mm. The

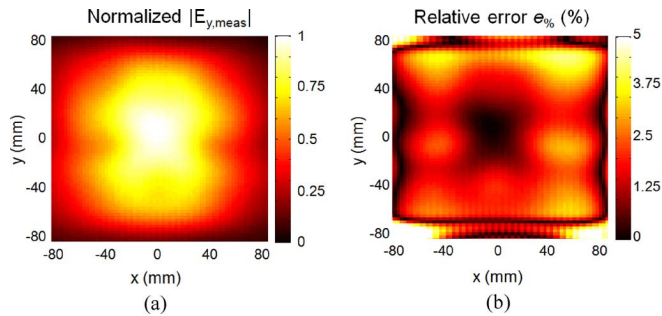


Fig. 6. (a) Normalized measured amplitude of the main component of the horn antenna at 4 GHz at 2 mm from its aperture; (b) probe relative error.

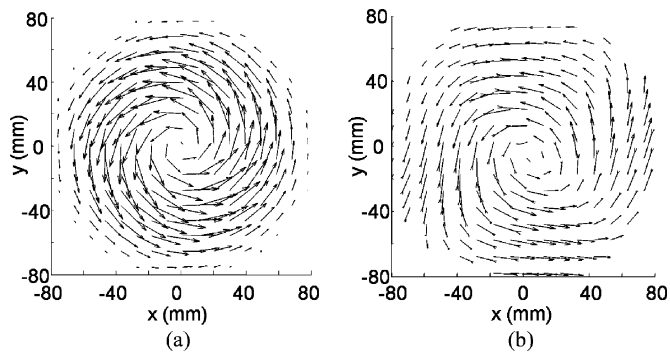


Fig. 7. Near-field vector patterns of the oversized waveguide at 6 GHz: (a) theoretical TE_{01} mode; (b) near-field scan at 2 mm from the aperture.

measurement setup consists of a PC-controlled xy -scanning system, with the probe directly connected to a Rohde&Schwarz ZVA50 network analyzer. The transversal field patterns have been then compared to the theoretical field distributions and some comparisons are here reported.

In Fig. 6(a) the measured near-field pattern of the main polarization E_y of the horn antenna is reported. The evaluation plane (xy) is 2 mm away from the probe and the scan is performed at 4 GHz. The scan grid has area of $(160 \times 160) \text{ mm}^2$ and a step resolution of 2 mm along x and y . To evaluate the accuracy of the probe to detect the desired field components, the normalized measured near-field has been compared to the known normalized theoretical distribution through a probe relative error $e_{\%} = \frac{||E_{y,meas}| - |E_{y,ideal}||}{|E_{y,ideal}|} \cdot 100$, plotted in Fig. 6(b). The error ranges from a value close to zero at the center of the measurement plane up to a maximum of 4.8% at the edges of the plane where the field is less intense and some diffraction effects from the borders of the horn antenna are occurring.

A second measurement has been performed on the near-field distribution of a circular pipe used for applications of radar level monitoring of liquid and solid materials contained in industrial vessels [10]. This measurement aims at showing the applicability of the proposed probe to a complex case. The pipe is nothing but an oversized circular waveguide where some modes can be excited by means of a mode converter connected to one of the two ends of the structure. The length of the sample waveguide was 1 m but, in normal application cases, the length of those pipes can reach 30 m or more, depending on the dimen-

sions of the vessel containing the material to be monitored. The near-field scan of the open aperture allows the determination of the field distribution inside the pipe, related to the propagating modes. In this case, two scans must be performed on the same grid in order to evaluate amplitude and phase of the two orthogonal transversal components. That information can be used to reconstruct the field vector pattern of the propagating wave inside the pipe. The field distribution in the pipe is a composition of several modes which are originally unknown. Indeed, the TE_{01} mode converter/launcher feeding the pipe excites, besides the dominant mode, a number of undesired modes. In Fig. 7(a) and (b), the theoretical TE_{01} distribution and measured multimode field distribution in a circular pipe at 6 GHz are, respectively, shown. The near-field scans have been performed with a resolution of 2.5 mm along x and y at a distance of 2 mm from the evaluation plane. The measured field in Fig. 7(b) predicts the existence of the TE_{01} mode in the multimode composition and shows the capability of the probe itself to correctly detect the x and y components of the electric field. The extracted pattern can be used to accurately characterize the mode composition inside the pipe.

V. CONCLUSION

An efficient 4-to-8 GHz-matched linear probe for near-field mapping of apertures and oversized waveguides has been demonstrated. The probe, based on a short dipole and an UWB feed, is able to provide a resolution smaller than 2.5 mm and a good rejection of undesired electric field components. Some near-field measurements of a horn antenna and an oversized waveguide showed how the probe can precisely reconstruct the E-field patterns of the structures under test.

REFERENCES

- [1] R. C. Johnson, H. A. Ecker, and J. S. Hollis, "Determination of far-field antenna patterns from near-field measurements," *Proc. IEEE*, vol. 61, no. 12, pp. 1668–1694, Dec. 1973.
- [2] D. M. Sheen, D. L. McMakin, and T. E. Hall, "Near field imaging at microwave and millimeter wave frequencies," in *IEEE MTT-S Int. Dig.*, 2007, pp. 1693–1696.
- [3] L. Bouchelouk, Z. Riah, D. Baudry, M. Kadi, A. Louis, and B. Mazari, "Characterization of electromagnetic fields close to microwave devices using electric dipole probes," *Int. J. RF Microw. Comput.-Aided Eng.*, vol. 18, no. 2, pp. 146–156, Mar. 2008.
- [4] S. Dieter and W. Menzel, "High-resolution probes for near-field measurements of reflectarray antennas," *IEEE Antennas Wireless Propag. Lett.*, vol. 8, pp. 157–160, 2009.
- [5] S. Dieter, Z. Yang, and W. Menzel, "A 77 GHz near-field probe with integrated illuminating waveguide," in *Proc. German Microw. Conf. (GeMIC)*, 2011, pp. 1–4.
- [6] K. Yang, G. David, S. V. Robertson, J. F. Whitaker, and L. P. B. Katehi, "Electrooptic mapping of near-field distributions in integrated microwave circuits," *IEEE Trans. Microw. Theory Tech.*, vol. 46, no. 12, pp. 2338–2343, Dec. 1998.
- [7] J. I. Moon and J. H. Yun, "The design of broadband probe for efficient near field measurements," *IEEE Antennas Wireless Propag. Lett.*, vol. 6, pp. 440–443, 2007.
- [8] M. Leib, M. Frei, and W. Menzel, "A novel ultra-wideband circular slot antenna excited with a dipole element," in *Proc. IEEE Int. Conf. Ultra-Wideband*, Vancouver, BC, Canada, Sep. 2009, pp. 386–390.
- [9] "CST Microwave Studio," CST Computer Simulation Technology AG, 2011.
- [10] N. Pohl, M. Gerding, B. Will, T. Musch, J. Hausner, and B. Schiek, "High precision radar distance measurements in overmoded circular waveguides," *IEEE Trans. Microw. Theory Tech.*, vol. 55, no. 6, pp. 1374–1381, Jun. 2007.